ELSEVIER

Clinical Biomechanics 16 Supplement No. 1 (2001) S111–S126

CLINICAL BIOMECHANICS

www.elsevier.com/locate/clinbiomech

Intradiscal pressure together with anthropometric data – a data set for the validation of models

Hans-Joachim Wilke [a,*], Peter Neef [b], Barbara Hinz [c], Helmut Seidel [c], Lutz Claes [a]

[a] *Institute for Orthopaedic Research and Biomechanics, University of Ulm, Helmholtzstrasse 14, 89081 Ulm, Germany*
[b] *Gesundheitspark, Ulm, Germany*
[c] *Federal Institute for Occupational Safety and Health, Berlin, Germany*

Abstract

Objective. To provide a database of intradiscal pressure measurements together with anthropometric data as basis for the validation of models that predict spinal loads.

Design. Intradiscal pressure was measured in a non-degenerated L4-5 disc of a volunteer. The anthropometric characteristics of this subject were extensively determined.

Background. Since it is usually impossible to quantify the load in the spine directly, it is predicted by various biomechanical models. However, they often cannot be validated because of the few in vivo data and missing anthropometric characteristics pertaining to them.

Methods. A pressure transducer (diameter 1.5 mm) was implanted in the nucleus pulposus of a non-degenerated L4-5 disc of a volunteer. Pressure was determined during exercises while standing, lifting activities, sitting unsupported on a stool or an ergonomic sitting ball, sitting in different postures and others. The anthropometric characteristics were determined using different tools.

Results. Pressure values: relaxed standing 0.5 MPa; standing flexed forward 1.1 MPa; standing extended backward 0.6 MPa; sitting unsupported 0.46 MPa; maximum values during lateral bending 0.6 MPa, during axial rotation 0.7 MPa, lifting a 20 kg weight with a round flexed back 2.3 MPa, with flexed knees 1.7 MPa, close to the body 1.1 MPa; sitting unsupported relaxed 0.45 MPa, actively straightening the back 0.55 MPa, with flexion 0.9 MPa; non-chalant sitting 0.3 MPa and others. Anthropometric characteristics with emphasis on data for the trunk are provided in tables.

Conclusions. Intradiscal pressure depends on the kind of preceding activity, posture, external loads and muscle activity.

Relevance

The data set can be used to verify a biomechanical model adjusted to the individual characteristics by a comparison of measured and predicted intradiscal pressures.

Keywords: Intradiscal pressure; Anthropometry; Trunk; Spine; Model; Verification

1. Introduction

Loading of the spine still is not well understood. It is, however, of great importance in the fields of orthopaedics, physiotherapy and ergonomics as overload is considered as one main risk factor for the degeneration of the disc. Usually it is not possible to quantify the spinal load directly because force transducers cannot be introduced into the spine of alive humans.

Therefore many computer models have been developed which try to simulate postures and activities to estimate the loads acting in the spine and may provide further information. Most have been attempts to estimate the load during lifting activities. First simplified models are known from Bradford and Spurling [1]. Many years later Morris et al. estimated the loads in the lumbar spine taking muscle forces from EMG measurements or intradiscal pressure or both into account [2,52,53].

Anthropometric data were seriously considered by Chaffin [3] who described the human body as a chain of rigid segments, which were connected by hinge joints.

McGill [4–6] developed more two-dimensional models for different symmetrical body positions and lifting

* Corresponding author.
E-mail address: hans-joachim.wilke@medizin.uni-ulm.de (H.-J. Wilke).

0268-0033/01/$ - see front matter
PII: S0268-0033(00)00103-0

conditions, also with muscle forces from EMG measurements. Others optimised the linked models for different lifting tasks of brick layers or nurses [7–10]. For asymmetrical lifting performances, three-dimensional models were introduced [11–16]. Other mathematical models were developed to simulate walking conditions [17–19].

Finite element models were created to investigate, for given lifting tasks, the stress in certain spinal structures. This can be done for single segment models [20,21] or for polysegmental models for static conditions [22–25]. Dynamical models are important for the understanding of whole body vibrations (WBV) which are particularly relevant in sitting postures [26,27].

The influence of muscles was often neglected and if they are taken into account they can be underestimated because little is known about their magnitude. The variation of trunk models as well as posture can have a strong effect on the predictions of muscle forces and spinal loading [28,29]. Also the effect of the abdominal pressure is discussed controversially [30].

Therefore most models cannot be validated, or even confirmed, because very few in vivo data exist, which provide absolute loading values, e.g., for the intradiscal pressure.

The most important data were provided from Nachemson's direct in vivo measurements in the 60s and 70s. In the first papers he reported absolute values in kg/cm^2 [31–36], later he presented them normalised to the standing posture [37]. Unfortunately anthropometric data are missing. Since then there have been few data to corroborate or dispute those findings.

Recently we measured intradiscal pressure again in vivo with a more advanced transducer than that used by Nachemson and complemented those earlier data with dynamic measurements and presented absolute values for different postures and exercises [38].

The purpose of this paper is to provide a database of anthropometric measures of the subject to complement the previously published new intradiscal pressure measurements which are summarised with pictures from videos. Additionally, previously not published pressures curves are provided. These data might enable an appropriate adjustment of computer models, to confirm them by a comparison of the predicted intradiscal pressure values with the measurements.

2. Methods

2.1. Pressure measurements

Due to the risks of this in vivo investigation, just one volunteer subject, a 45 year old male orthopaedist in good physical condition with no previous history of back pain could be studied. This experiment was approved in this single instance by the state ethical review board (Landesärztekammer Baden-Württemberg, Germany).

The protocol allowed the selection of one intervertebral disc for the implantation of the transducer. Since intradiscal pressure can only be reliably measured in a non-degenerated disc, we used MRI to evaluate the viability of the lumbar discs of the subject. Based on these findings we chose the L4-5 disc, which did not show any signs of degeneration or dehydration. After preparation with antibiotics in order to reduce the risk of infection, a flexible pressure transducer with a diameter of 1.5 mm was implanted from a dorsolateral transforaminal approach into the centre of the intervertebral disc (Figs. 1a and b). This procedure was performed under local anaesthesia. Details about the technique are described in the previous paper [38].

Pressure was measured with a telemetry system over a period of about 24 h. Most exercises were recorded with a sampling rate of 300 Hz (samples per second). Pressure values in the previous paper were reported for following situations: various lying positions, sitting positions in a chair, in an armchair, during sneezing, laughing, walking, stair climbing, load lifting, hydration over 7 h of sleeping and others.

Most exercises were simultaneously registered on videotape, on photographs, and some additionally quantified by a motion analysis system.

In this paper we want to report exercises from which certain postures could be used to confirm results from computer-models. The first data are motions in the standing position which were quantified by an additional motion analysis system. For these measurements the volunteer was asked to flex and extend, to flex laterally to the right and the left, and to rotate to the right and the left as much as possible. All motions were started from the neutral position, defined when he was standing relaxed. During these exercises intradiscal pressure was recorded and the mobility of the lumbar spine between the sacrum and the thoracolumbar junction was assessed using an ultrasound based motion analysis system (Zebris CMS50, Isny, Germany) (Fig. 1(c)).

This paper also presents pictures taken from video sequences with the respective pressure values for lifting tasks, sitting positions in a stool without backrest, an armchair with backrest. To complement these more or less static sitting positions dynamic measurements on a pezzi-ball (ergonomic sitting ball) were carried out during jumping which resembles self-generated periodic whole body vibration at about 1 Hz.

2.2. Anthropometric measurements

A disc area of 18 cm^2 was determined from the mid-horizontal MRI-scan, which was taken four weeks before the intradiscal pressure measurements.

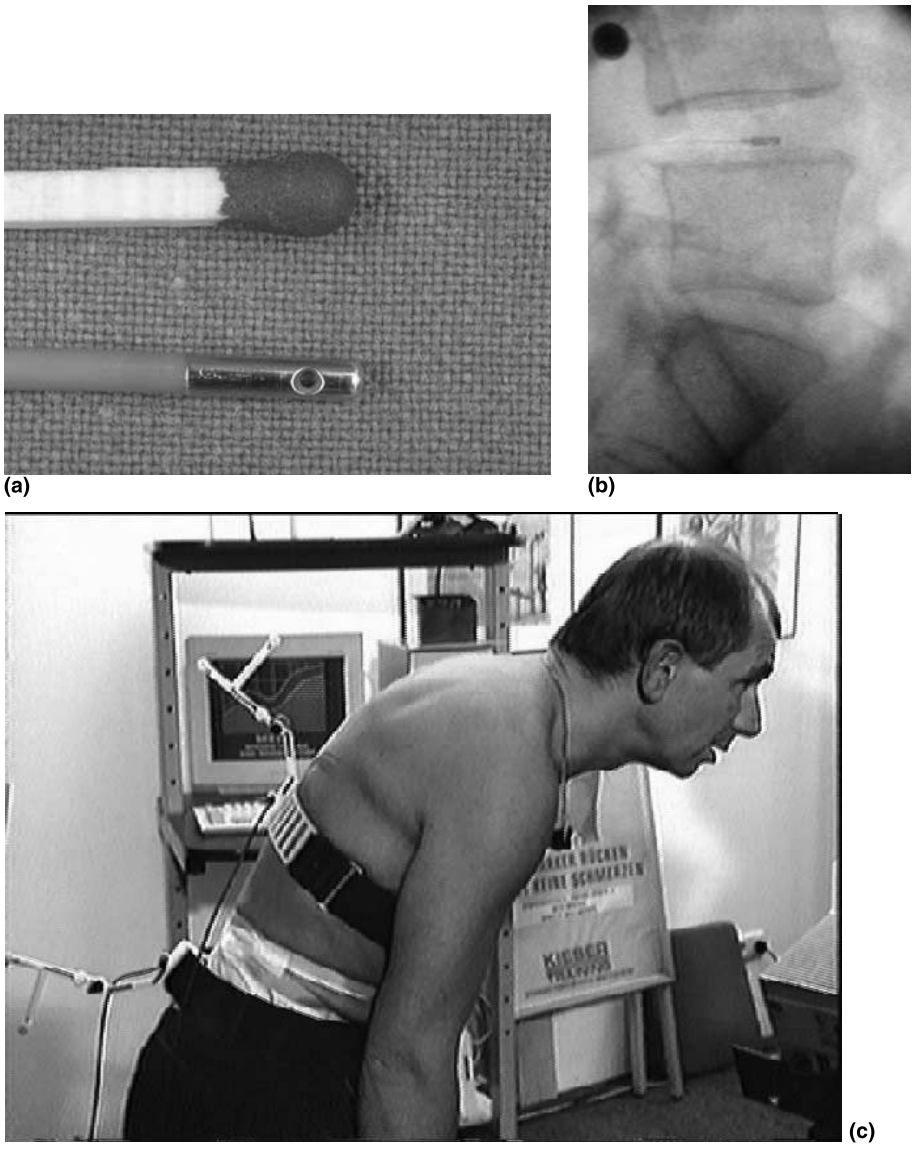

Fig. 1. Intradiscal pressure measurements in vivo. (a) Pressure transducer for the intradiscal pressure measurements in vivo. (b) Pressure transducer after implantation in L4/5 for the intradiscal pressure measurements in vivo. (c) In vivo recording of the intradiscal pressure and the motion between sacrum and thoracolumbar junction was performed with one volunteer.

About two years after the study, the anthropometric status of this subject was extensively determined (Measurement instrumentation by Siber Hegner Machinery, Switzerland; details see Appendix A). The body mass of the subject was measured by weighing the lightly clothed body with a Soehnle scale (precision 0.15 kg). The measurements were performed with the nearly unclothed body, in basic positions, and on the right side for symmetric measures. Basic positions are defined for standing and sitting [39]. These definitions are necessary for the reproducibility of the measurements. The basic position for standing is an upright erect posture which the subject can maintain constant during the measurements. The body mass should be equally distributed on both feet, with both heels touching each other and the points of the feet diverging slightly. The knee- and hip joints are stretched. The pelvis and the spine are tensed erect, but not overstretched. The shoulder girdle is held loosely. Arms and hands hang stretched at the sides of the body with the palms turned medially. The ear–eye plane of the head is orientated horiziontally and kept without muscular effort. In the basic sitting posture the subject is sitting with an erect pelvis and an extended spine on a horizontal, incompressible seat surface. The shoulder girdle is held slackly and the shoulders must not be raised. The thighs are placed in parallel on the seat area. The shanks are at a right angle to the seat and the whole soles contact the reference surface. The definitions of measurements and measuring devices are described in the Appendix A.

Detailed measurements were performed for the abdomino-thoracic part of the trunk in the basic standing

posture. This part ranged over 71.5 cm from the cervical height (149.2 cm above the floor) to the perineal height (77.7 cm above the floor, definitions see Appendix A). It was subdivided into 10 horizontal segments with an identical height of 1/10 stem length (7.1 cm) as recommended earlier [40]. In order to minimise the measuring errors, the upper height of each segment was marked on the skin ventrally and dorsally. In the basic sitting posture, the measurements were performed only for the accessible markers. Since the segments in this posture did not remain horizontally, the height of each slice was measured dorsally and ventrally with reference to the floor. The height of the seat surface above the floor amounted to 45.6 cm. Skinfolds were measured according to [41].

3. Results

3.1. Intradiscal pressure measurements in vivo

In a previous study pressures were reported for daily activities [38]. Some of them are repeated here. We found for lying in prone position 0.1 MPa, lying laterally 0.12 MPa, relaxed standing 0.5 MPa, standing flexed forward 1.1 MPa, sitting unsupported 0.46 MPa, sitting with maximum flexion 0.83 MPa, non-chalant sitting 0.3 MPa, lifting a 20 kg weight with round flexed back 2.3 MPa, with flexed knees 1.7 MPa, and close to the body 1.1 MPa. During the night, pressure increased from 0.1 to 0.24 MPa.

The pressure curves reported here are to complement those postures and activities which might be useful for modelling.

3.1.1. Exercises while standing

In relaxed standing, intradiscal pressure in vivo was reproducible around 0.43–0.50 MPa. The pressure changed depending on the motion (Fig. 2). The pressure curves were very similar when repeating the exercises.

We observed the most pronounced change in flexion, the pressure increased almost linearly to 1.08 MPa at a flexion angle of 36° between the thoracolumbar junction and the sacrum (Fig. 2(a)). In extension there was also a linear increase, but only up to 0.6 MPa at an angle of 19°.

Lateral bending showed, roughly, a symmetrical behaviour (Fig. 2(b)). The pressure increased linearly up to 0.59 MPa at an angle of 18° to the right and 23° to the left. Interestingly, beyond these ranges the pressure decreased on both sides to a lower value of about 0.38 MPa at an angle of about 29°. Probably up to the angle of 20° the muscles tried to stabilise the spine actively. Then the muscles released and the spine was only stabilised passively, which interestingly resulted in a pressure decrease.

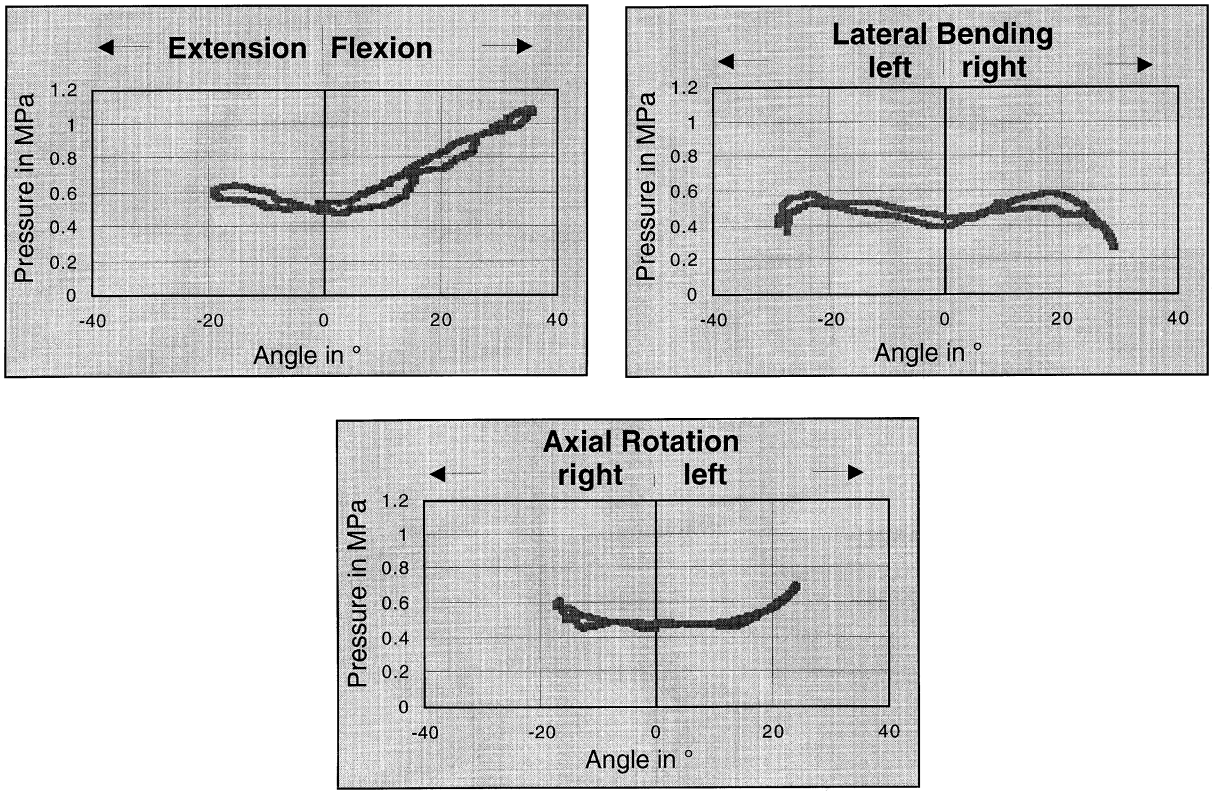

Fig. 2. Intradiscal pressure in vivo in the segment L4/5 with respect to total motion between the thoracolumbar junction and the sacrum.

In axial rotation the pressure also increased with twisting (Fig. 2(c)). Here our volunteer was able to twist further to the left then to the right. The pressure increased to 0.7 MPa at 24° to the left and to 0.6 MPa at 17° to the right.

3.1.2. Lifting activities

The highest pressure range was found during lifting and carrying a full crate of beer (height × width × depth = 300 × 400 × 300 mm^3) with a weight of 19.8 kg (Fig. 3). Lifting and lowering the case with both hands in front of the body and with knees bent and in upright posture, with actively extended back as taught in some back schools, increased the pressure from 0.5 MPa with quiescent standing to 1.72 MPa during lifting and or 1.68 MPa during lowering (Fig. 3(a)). Lifting the case by bending over with the legs almost straight increased the pressure up to 2.3 MPa (Fig. 3(b)). In comparison the

Fig. 3. Lifting activities: (a) lifting as taught in back schools; (b) lifting bent over with round back; (c) exercise finger tip – floor distance; (d) crate of beer held close at chest level; (e) held away about 60 cm; (f) walking with one crate (mean value); (g) lifting two crates; (h) walking with two crates (mean value).

finger tip to floor exercises creates a pressure of 1.6 MPa (Fig. 3(c)). Holding the case close to the body at chest level produced a pressure of about 1.0 MPa (Fig. 3(d)), whereas holding it 60 cm away from the chest increased the pressure to 1.8 MPa (Fig. 3(e)). Lifting this case with one hand on the side created a pressure of 2.1 MPa, carrying it laterally either in the right or in the left hand leads to a pressure of 1.0 MPa in the L4-5 disc (Fig. 3(f)). The maximum pressure when lifting two cases at the same time was 2.1 MPa (Fig. 3(g)) and carrying them symmetrically in two hands created only a pressure of about 0.9 MPa (Fig. 3(h)).

3.1.3. Sitting unsupported on a stool or an ergonomic sitting ball

In sitting, fluctuations in pressure occurred with changes in posture and support. Relaxed sitting on a stool with a normally straight back produced a pressure peak region of 0.45 to 0.50 MPa (Fig. 4(a)), similar to standing. Bending forward about 20° with straight back and without arm support increased the pressure to 0.63 MPa (Fig. 4(b)), further bending forward increased the pressure up to 0.83 MPa, supporting the elbows on thigh in this position in order to relax, reduced the pressure to 0.43 MPa (Fig. 4(c)). Sitting unsupported strongly relaxed in flexed position with the head in front of the body created a pressure 0.90 MPa (Fig. 4(d)).

Similar pressures were found on an ergonomic sitting ball. In the upright position the pressure was 0.5 MPa (Fig. 4(e)), when jumping in this position it cycled between 0.4 and 0.6 MPa (Fig. 5). In a relaxed and slightly flexed position, it equalled about 0.65 MPa (Fig. 4(f)). When jumping in this position the amplitude ranged between 0.55 and 0.75 MPa (Fig. 5(a)) and reached a maximum between 0.6 and 0.8 MPa with jumping in a strongly relaxed flexed position (Fig. 5(b)) which might be compared with an unsupported and strongly relaxed position in a construction vehicle going over bumps; in both cases a and b the displacement was similar with 60 mm $\pm$ 10 mm at a frequency of about 1.7 jumps per second. However, different motor control mechanisms

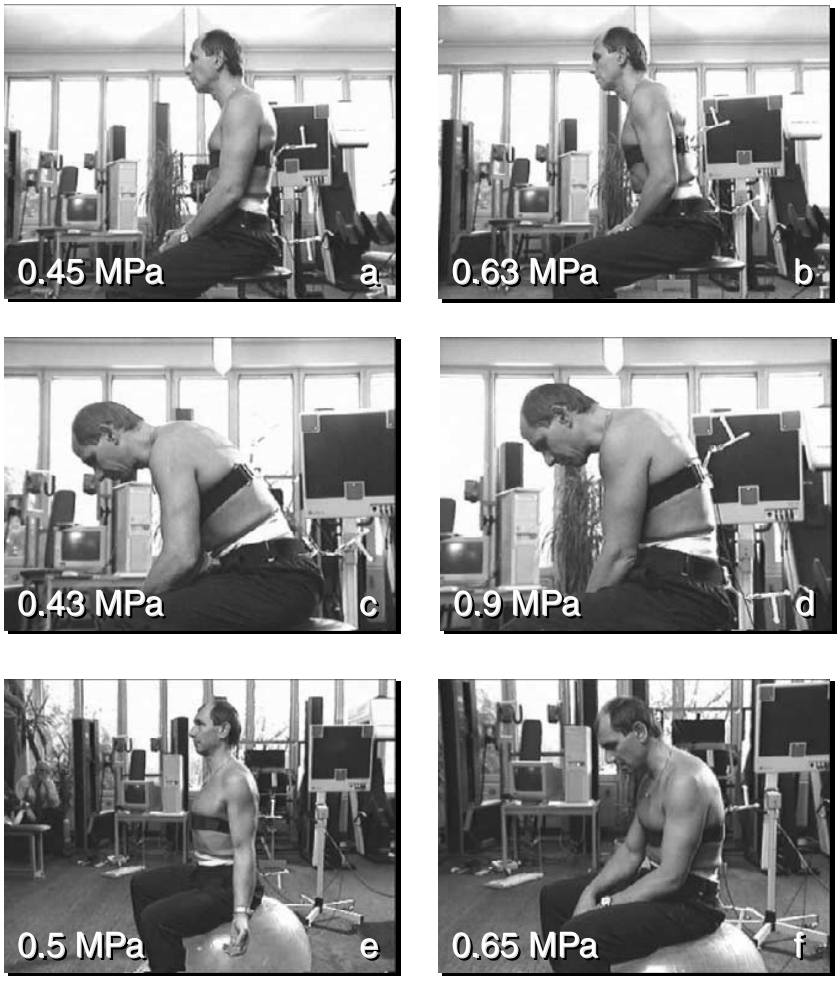

Fig. 4. Unsupported sitting: (a) relaxed erect sitting; (b) erect sitting bent forward; (c) flexed forward with elbows on thigh (d) flexed actively forward; (e) sitting on an ergonomic sitting ball with straight back; (f) sitting on an ergonomic sitting ball in flexed posture.

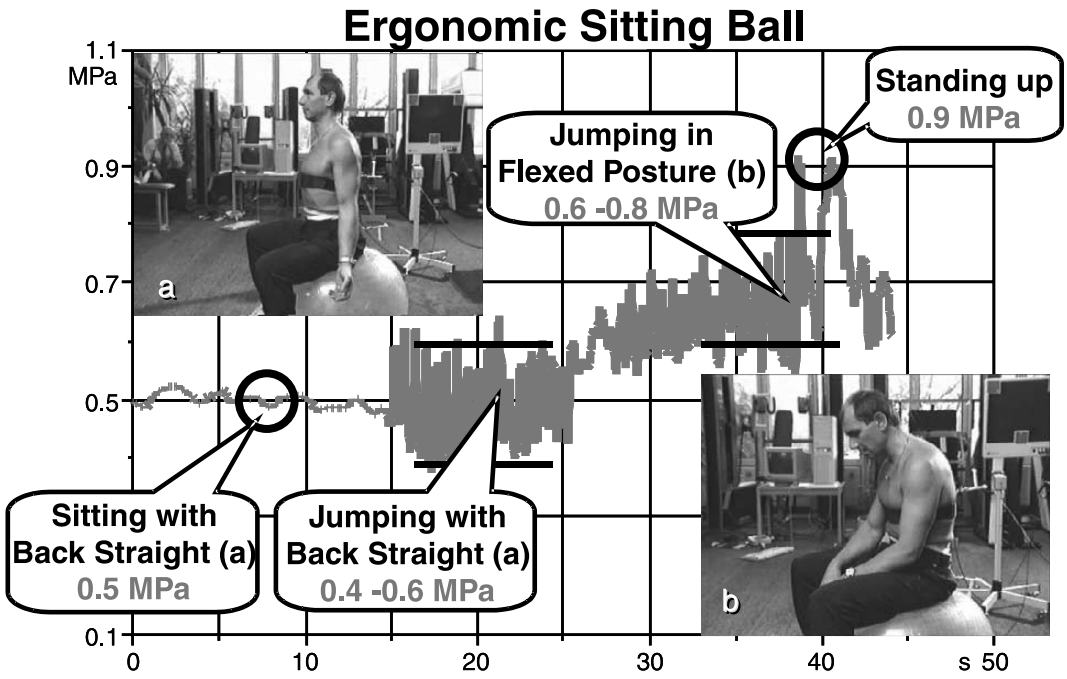

Fig. 5. Intradiscal pressure during sitting and jumping on an ergonomic sitting ball.

during self-generated and forced whole-body vibration [42] suggest different internal loads.

3.1.4. Sitting in an armchair

By changing the sitting in an armchair the pressure can be varied in manifold ways. Under the condition of leaning backwards with about 15° the pressure is decreased to 0.33 MPa (Fig. 6(a)). The lower the subject slouched into the chair, the more the pressure decreased (to a minimum of 0.27 MPa), despite further increasing the flexion in his back (Fig. 6(b)). Supporting the stretched legs on a stool increased the pressure slightly to 0.38 MPa (Fig. 6(c)). A similar increase was found by putting the arms across the chest (Fig. 6(d)). Sitting relaxed without backrest in an almost upright position created a pressure of 0.44 MPa (Fig. 6(e)) as on the stool or on the ergonomic sitting ball. In all these sitting postures the pressure was lower than 0.48 MPa as found for relaxed standing (Fig. 6(g)). The only exception where the pressure was higher compared to standing with 0.55 MPa occurred when sitting consciously erect actively straightening and extending the back, as taught in some back schools (Fig. 6(f)). Standing up from the chair and sitting down led to a pressure peak of 1.1 MPa. Body lifting by armsupports decreased the pressure only to only 0.1 MPa.

3.2. Anthropometric measures

Tables 1 and 2 present the data of the 10 trunk segments in the standing and sitting postures, respectively.

The majority of measures are listed separately for the standing and sitting postures in the second column of the Appendix A. The skin folds are also presented in the Appendix A. For the standing posture the anthropometric measures are classified as heights, breadths, depths, and circumferences. The third column presents the results of Greil [43] for the 50th percentile (P 50) of the German male population with the corresponding age (45–49 years). The body mass of the subject was measured by weighting the lightly clothed body with a Soehnle scale (precision 0.15 kg). The body mass amounted to 72 kg. The body mass of P 50 equalled 78.5 kg [43].

4. Discussion

This paper provides a database of intradiscal pressures for a number of exercises during standing, lifting activities and many different sitting postures together with anthropometric data which might serve as basis for the validation of mathematical models that predict spinal loads under static and dynamic conditions.

Until now models had to be confirmed with the data provided from Nachemson's pressure measurements in the 60s and 70s. Unfortunately, anthropometric data were missing in his papers. Therefore his absolute values in kg/cm^2 reported in the first papers [31–36] or the normalised results [37] can only be used for a rough estimation.

In the present paper the absolute pressure values measured in the centre of L4-5 are reported for the first

Fig. 6. Sitting postures in an armchair: (a) relaxed erect sitting with backrest; (b) slouched sitting; (c) slouched sitting with legs supported; (d) slouched sitting with arms across the chest; (e) relaxed erect sitting without backrest; (f) sitting actively staightening the back; (g) relaxed standing; (h) body lifting by arm supports.

time together with many anthropometric data that can be used to model individually our volunteer Peter Neef (Appendix A). Additionally we provide detailed data about the measures of 10 equal horizontal disc segments of the upper trunk in the standing and sitting posture to model the upper trunk of our subject.

During many exercises we found a good correlation with Nachemson's data, but not in the comparison of standing and sitting or of the various lying positions [38]. These differences between ours and Nachemson's results may be explained by the use of different transducers. Although this study was only performed with one subject, it confirmed results from an indirect method using the stadiometry [44], and were also found shortly after the new intradiscal pressure measurements with an instrumented spinal fixator [45] and new sta-

Table 1
Measures of 10 horizontal trunk segments of the upper trunk in the standing posture

Trunk segment No.	Body height from the reference surface (cm)	Breadth (cm)	Depth (cm)	Circumference (cm)
1	149.2	16.9	12.0	38.0
2	142.1	39.2	14.0	97.0
3	134.9	43.2	20.6	109.7
4	127.8	28.6	21.5	98.5
5	120.6	28.1	20.5	88.5
6	113.4	27.1	20.0	84.0
7	106.3	29.0	19.0	83.2
8	99.2	31.5	21.0	88.5
9	92.0	33.1	20.2	93.5
10	not measurable	not measurable	not measurable	not measurable

Table 2
Measures of 10 horizontal trunk segments of the upper trunk in the sitting posture

Trunk segment No.	Height ventral from the reference surface (cm)	Height dorsal (cm)	Breadth (cm)	Depth (cm)	Circumference (cm)
1	108.3	113.6	17.0	13.0	37.0
2	103.2	105.8	35.7	14.0	98.0
3	95.0	98.7	41.0	20.2	108.9
4	87.9	91.0	32.0	21.5	97.0
5	80.2	84.3	29.5	20.6	89.5
6	72.5	76.9	26.7	21.3	84.0
7	66.0	69.8	29.7	20.3	85.0
8	not measurable	61.0	34.0	21.8	89.0
9	not measurable	51.0	37.0	not measurable	96.0
10	not measurable	not measurable	not measurable	not measurable	not measurable

diometry measurements [46]. Using the latest technology, this study indicated that: intradiscal pressure during sitting may in fact be less than that in erect standing; muscle activity increases pressure; constantly changing position is important to hydrate and dehydrate the disc; and, physiotherapy methods are valid in many cases but should be re-evaluated in some others [38].

Our subject Peter Neef is representing a well-trained person whose anthropometry lies in the 50th percentile of the German male population, aged between 45 and 49 years. He belongs to the intermediate type of robustness of the skeleton [43]. The shares of active body mass and fat amounted to 63.5 and 8.5 kg, respectively [47]. We determined a disc area of 18 cm^2 from an MRI scan, which can slightly differ from the real value due to the voxel error, or if we did not evaluate exactly the mid-disc plane. Anthropometric data can be used to predict the area of the disc [48]. The prediction based on the body mass resulted in 19.36 cm^2 for the disc L4-5, that based on the stature and diameters of the wrist, elbow, ankle and knee, in 23.97 cm^2.

Although the anthropometric data were determined only two and a half years after the actual pressure measurements, we believe that this is no problem because our volunteer Peter Neef did not change in the meantime. He is a very well-trained person who is exercising regularly and his weight stayed almost constant during this period. His weight was 70 kg when we performed the measurements and 72 kg when we took the anthropometric data. Bodyweight and his height, which was reported in the previous paper are the data he told us during the measurements. The data reported in the present paper were measured by the authors themselves with the described methods (Appendix A). Therefore the data reported in this paper are probably more reliable than the height and weight described earlier.

The detailed data of the trunk segments may help to improve the distribution of the most significant partial masses in the model. The skin fold data could be used to specify the part of the ''wobbling mass'', if such mass is to be implemented in a model [49].

Often researchers are interested in absolute force values. However, we preferred not to convert the absolute pressure data (MPa) into force values (Newton). The reason is that it is still not quite clear how to convert these data. Nachemson described pressure profiles from in vitro experiments [34] whose constant maximum was

only in the nucleus decreasing linearly to zero over the entire annulus of a normal disc. The pressure profile stays constant over the entire disc for moderately degenerated discs, and it may even show the opposite trends to the normal disc if it is severely degenerated. This, however, was not supported by the in vitro profilometry studies [50,51] which showed an almost constant plateau over the entire nucleus and most of the annulus. Only in the outer layers or the outer 3–5 mm of the annulus the pressure is dropping down to atmospheric pressure. An inhomogeneous pressure distribution with a peak in the posterior annulus was found for degenerated discs.

Many of our exercises are recorded on video. Unfortunately, the recordings were not standardised, in the sense that we did not attach markers on the body of the subject. In addition, the camera position was not constant. Furthermore, there were no pure sagittal recording. However, sophisticated software packages might be able to extract from the different video frames time-curves of joint positions or points at the crate of beer.

Although, this study was limited to only one subject due to the risk of this method these pressure values provide inimitable data for the validation of computer models adjusted to individual anthropometry.

Acknowledgements

The authors wish to thank Dr. Thomas Hoogland for the implantation of the pressure transducer, Bernd Sigl for technical support, Reinholde Langer and Ulrike Zürn the physiotherapists from our physiotherapy school in Ulm, Dipl.- Ing. Jürgen Marx, Toni Negele for the measuring technique and Karl Maute for Video assistance.

The study was financially supported by Kieser Training AG, Zurich, Switzerland. Some collaborative aspects of this research were supported by the European Commission under BIOMED 2 concerted action BMH4-CT98-3251 (Vibration Injury Network).

Appendix A. Anthropometric measurements for our subject in comparison to the 50th-percentile (P50) – results, definitions and equipment

More detailed explanation of the above measures:

Anthropometer – AM, beam compasses – BC, sliding calipers – SC, large calipers – LC, calipers – C, tape measure – TP

A.1. Standing posture/heights

Body height. Linear distance of the vertex (highest point of the top of the head in the median plane with the

Anthropometrical parameter	Subject (cm)	P50 (cm)
Body height	173.9	171.7
Comfortable body height	172.2	
Height to the external occipital protuberance	163.0	
Ear height	160.1	158.4
Chin height	150.8	149.6
Height to bridge of the nose	162.1	
Cervical height	148.1	147.8
Inferior height of the scapula	122.5	
Height of the base of the neck	142.3	
Deltoid height	132.5	
Upper sternal height	139.5	141.0
Lower sternal height	122.4	
Shoulder height	140.4	141.6
Dorsal height of the base of the arm	130.0	
Height of the waist	108.8	
Height of the umbilicus	103.2	
Height of the largest breadth of the hip	96.8	
Height of the elbow joint	107.1	105.8
Wrist height	84.4	
Height of the middle finger tip	64.5	
L3 Height	109.0	
L4 Height	105.0	
L5 Height	102.5	
Height of the iliac crest	106.3	
Iliospinal height	98.0	98.4
Symphysion height	89.2	
Height of the greater trochanter	93.4	
Height of the posterior gluteal point	87.7	
Height of the perineum	77.7	
Knee height	46.3	46.6
Height of the ankle	9.6	
Foot length	27.0	26.6
Foot breadth	10.4	9.7
Ankle breadth	7.1	
Knee breadth	10.1	10.1
Elbow breadth	7.3	7.2
Wrist width	6.1	
Shoulder breadth	37.6	40.0
Bi-deltoidal shoulder width	44.3	47.5
Chest breadth	27.5	31.2
Breadth of the waist	27.1	
Breadth of the back contour	36.2	
Pelvic breadth	28.3	30.7
Spinal breadth	24.9	

Anthropometrical parameter	Subject (cm)	P50 (cm)
Hip breadth	33.1	35.1
Bi-trochanteric breadth	33.3	37.0
Maximal head length	19.4	18.9
Maximum head breadth	16.1	15.9
Upper trunk depth	14.8	
Chest depth	21.2	
Xyphoid depth	23.0	24.0
Bi-deltoid body circumference	108.5	
Great chest circumference	97.0	
Chest circumference	94.5	
Horizontal chest circumference	90.5	102.7
Circumference of waist	83.0	
Minimum circumference of waist	80.0	95.5
Circumference of the body at elbow height	81.0	
Upper circumference of the pelvis	83.0	
Circumference of the body at the height of the wrist joint	95.0	
Bi-trochanteric circumference	94.0	
Maximum circumference of the hips	95.4	
Transversal cranial bend	31.0	36.2
Head circumference	58.5	57.8
Neck circumference	38.0	39.8
Circumference of the base of the upper arm	34.0	
Relaxed upper arm circumference	32.2	
Contracted upper arm circumference	35.5	
Circumference of the elbow	28.5	
Maximum forearm circumference	30.0	28.0
Minimal forearm circumference	19.5	
Wrist circumference	18.7	
Circumference of the base of the thigh	57.0	
Circumference of the thigh	57.4	
Lowest circumference of the thigh	45.0	
Circumference of the knee	40.0	
Circumference of the shank	38.0	
Minimum circumference of the shank	23.2	
Middle circumference of the foot	25.4	
Height of seat surface	45.6	
Seated height	89.3	89.9
Relaxed seated height	86.4	
Height to the acromion sit.	57.2	60.0
Inferior height of the scapula sit.	41.9	45.0
Height of the waist sit.	25.2	
Height of the umbilicus sit.	21.7	
Height of the pelvis sit.	22.1	24.0
C7 Height sit.	65.5	66.1
L3 Height sit.	23.0	
L4 Height sit.	20.1	
L5 Height sit.	15.0	
Iliospinal height sit.	14.6	
Height of the elbow joint sit.	25.9	24.0
Height of the iliac crest sit.	22.3	
Height of the edge of the thigh	13.2	
Height of the knee sit.	56.0	53.6
Greatest width across the hips sit.	38.0	
Greatest sagittal diameter of the abdomen sit.	28.0	
Buttocks – knee – length	58.9	60.6
Skinfolds		
Skin fold thick when standing (cm) (Gauge : GPM skin fold gauge)		
On the cheek, before the tragus	6.4	
Under the jaw above the hyoid bone	5.1	
Front arm pit fold	3.3	
Over the 10th rib in the anterior axillary line	8.1	
Abdomen – in the first quarter of the distance between the umbilicus and front upper iliac crest	7.1	
Outside the anterior superior iliac spine	4.8	
Below the shoulder blade angle	7.4	20
Over the triceps muscle	8.3	14
Over the m. rectus femoris at the transition to the knee tendon	9.5	

head orientated in the plane of the ear and eyes) from the reference surface in an upright posture – AM

Comfortable body height. Linear distance of the vertex (highest point of the top of the head in the median plane with the head orientated in the plane of the ear and eyes) from the reference surface in comfortably relaxed posture – AM

Height to the external occipital protuberance. Linear distance of the external occipital protuberance (upper nape point, corresponds to the furthest projecting point of the external occipital protuberance at the boundary between rear of the head and the nape) from the reference surface – AM

Ear height. Linear distance of the tragus (ear point; that point at which the upper edge of the cartilage projection which partially covers the entrance to the ear joins the base of the ear) from the reference surface – AM

Chin height. Linear distance of the symphysis (corresponds to the deepest, therefore caudal point of the lower jaw in the median plane) from the reference surface – AM

Height to bridge of the nose. Linear distance of the point where the frontonasal suture crosses the median line, from the reference surface – AM

Cervical height. Linear distance of the most dorsal point of the tip of the spinous process of the seventh cervical vertebra from the reference surface AM

Inferior height of the scapula. Linear distance of the inferior angle of the scapula from the reference surface – AM

Height of the base of the neck. Linear distance of the highest point of the lateral part of the clavicula from the reference surface – AM

Deltoid height. Linear distance of the most lateral point of the upper arm in the area of the musculus deltoideus from the reference surface – AM

Upper sternal height. Linear distance of the deepest point of the upper dorsal border of the manubrium in the mid-sagittal plane from the reference surface – AM

Lower sternal height. Linear distance of the most distal point of the xiphoid process in the mid-sagittal plane from the reference surface – AM

Shoulder height. Linear distance of the acromion process (corresponds to the most lateral point of the shoulder blade at the top of the shoulder) from the reference surface – AM

Dorsal height of the base of the arm. Linear distance of the most cranial point of the dorsal arc of the fossa axillaris from the reference surface – AM

Height of the waist. Linear distance of the most medial point of the lateral curvature of the trunk in the area of the transversus abdominis muscle from the reference surface – AM

Height of the umbilicus. Linear distance of the middle of the umbilicus from the reference surface – AM

Height of the largest breadth of the hip. Linear distance of the most lateral point in the region lateral to the hip joint from the reference surface – AM

Height of the elbow joint. Linear distance of the most proximal part of the head of the radius from the reference surface, measuring position: out stretched arm, palms to the thigh – AM

Wrist height. Linear distance of the most distal point of the styloid process of the radius from the reference surface – AM

Height of the middle finger tip. Linear distance of the most distal point of the tip of the middle finger from the reference surface for outstretched, downward hanging arms and fully extended hands, whose longitudinal axis must be in the extension of the forearm axis, palms to the side of the thigh – AM

L3 Height. Linear distance of the most dorsal point of the spinous process of the third lumbar vertebra from the reference surface – AM

L4 Height. Linear distance of the most dorsal point of the spinous process of the fourth lumbar vertebra from the reference surface – AM

L5 Height. Linear distance of the most dorsal point of the spinous process of the fifth lumbar vertebra from the reference surface – AM

Height of the iliac crest. Linear distance of the most cranial part of the iliac crest from the reference surface – AM

Iliospinal height. Linear distance of the furthest ventrally and distally directed point of the anterior superior iliac spine from the reference surface – AM

Symphysion height. Linear distance of the upper edge of the pubic symphysis from the reference surface – AM

Height of the greater trochanter. Linear distance of the most proximal part of the greater trochanter of the femur from the reference surface – AM

Height of the posterior gluteal point. Linear distance of the most dorsal point in the area of the musculus gluteus maximus from the reference surface – AM

Height of the perineum. Linear distance of the most distal point of the medial base of the thigh from the reference surface – AM

Knee height. Linear distance of the most proximal point of the medial upper edge of the medial condyle of the tibia from the reference surface – AM

Height of the ankle. Linear distance of the most distal point of the medial (tibial) malleolus from the reference surface – AM

Foot length. The projected distance relative to the longitudinal axis of the foot between the most dorsal point of the heel for a loaded foot and the most distal point of the first or second toe (ignoring the toe nail) with the foot partially bearing weight and the toes relaxed – BC

A.2. Standing posture/breadth

Foot breadth. The projected distance relative to the longitudinal axis of the foot between the most lateral point of the lateral edge of the foot near the fifth metatarsophalangeal joint and the most medial point of the inner edge of the foot in the region of the first metatarsophalangeal joint – BC

Ankle breadth. Linear distance between the most medial point of the medial (tibial) and the most lateral point of the lateral (fibular) malleoli, i.e., between the most lateral point of the outer ankle and the most medial point of the inside ankle – SC

Knee breadth. Linear distance between the most medial point of the medial epicondyle of the femur and the most lateral point of the lateral epicondyle – SC

Elbow breadth. Linear separation between the most lateral point of the lateral epicondyle of humerus and the most medial point of the medial epicondyle of humerus, i.e., between the most lateral and medial points of the upper arm in the region of the elbow joint – SC

Wrist width. Diameter between the most prominent points of the styloid processes of the radius and the ulna – SC

Shoulder breadth. Linear distance between the most lateral points of the two acromion processes – LC

Bi-deltoidal shoulder width. Greatest transverse diameter between the most lateral points in the area of the deltoid muscles – LC

Chest breadth. Greatest transverse diameter of the torso at the height of the middle of the sternum where the fourth pair of ribs articulate the sternum, when breathing softly – LC

Breadth of the waist. Linear distance between the right and left most medial points of the lateral contours of the trunk in the region of the transverse muscle of abdomen – LC

Breadth of the back contour. Linear distance between the two most cranial points of the dorsal arcs of the fossae axillares – LC

Pelvic breadth. Linear distance between the two most lateral parts of the iliac crests – LC

Spinal breadth. Linear distance between the two furthest ventrally and distally directed points of the anterior superior iliac spine – LC

Hip breadth. Greatest transverse diameter of the torso in the region of the hips; distance between the two most lateral points in the hip and thigh regions – LC

Bi-trochanteric breadth. Linear distance between the two most proximal points of the greater trochanters of the femoral bones – LC

Maximal head length. Linear distance from the opisthcranion (craniometric point situated on the occipital bone at its most posterior point in the midline) to the glabella (point in the midline of the frontal bone at the most prominent point between the medial ends of the superciliary arches) – C

Maximal head breadth. Linear distance between the two most lateral points of the cranium cerebrale – C

A.3. Standing posture/Depths

Upper trunk depth. Distance between the deepest point of the upper dorsal border of the manubrium in the mid-sagittal plane and the most dorsal point of the tip of the spinous process of the seventh cervical vertebra – LC

Chest depth. Greatest sagittal diameter of the torso at the height of the middle of the sternum (cf. chest breadth) – LC

Xiphoid depth. Sagittal diameter of the torso at the most distal point of the xiphoid process in the mid-sagittal plane (cf. lower sternal height) – LC

A.4. Standing posture /Circumferences

Bi-deltoidal body circumference. Horizontal circumference at the height of the most lateral points in the area of the deltoid muscles – TP

Great chest circumference. Circumference of the upper torso at the inferior angles of the scapulae and the nipples – TP

Chest circumference. Horizontal circumference of the upper torso at the height of the middle of the sternum – TP

Horizontal chest circumference. Circumference of the upper torso at the height of the nipples – TP

Circumference of waist. Horizontal circumference of the torso at the height of the middle of the umbilicus when breathing softly – TP

Minimum circumference of waist. Smallest horizontal circumference of the torso between the chest and hips when breathing softly – TP

Circumference of the body at elbow height. Horizontal circumference of the upper torso at the height of the most dorsal and distal point of the olecranon (the point is identified, when the forearm is flexed by 90 degrees to the upper arm) – TP

Upper circumference of the pelvis. Horizontal circumference of the torso at the height of the most cranial part of the iliac crest – TP

Circumference of the body at the height of the wrist joint. Horizontal circumference of the torso at the height of the most distal point of the styloid process of the ulna – TP

Bi-trochanteric circumference. Horizontal circumference of the torso at the height of the most lateral points of the greater trochanters of the femoral bones – TP

Maximum circumference of the hips. Horizontal circumference of the torso at the height of the most dorsal points in the area of the greatest gluteal muscles – TP

Transversal cranial bend. Bend in the frontal plane from the point where the upper edge of the tragus joins the base of the ear to that point on the other side – TP

Head circumference. Roughly horizontal circumference of the head measured over the glabella and opisthocranion (cf. maximal head length) – TP

Neck circumference. Smallest circumference of the throat with the head held in the plane of the eyes and ears – TP

Circumference of the base of the upper arm. Upper arm circumference at the height of the most cranial point of the dorsal arc of the fossa axillaris with the arm hanging loosely and measured normal to the longitudinal axis of the upper arm – TP

Relaxed upper arm circumference. Greatest upper arm circumference with the arm hanging down and the muscles relaxed, measured normal to the longitudinal axis of the upper arm – TP

Contracted upper arm circumference. Upper arm circumference with a flexed arm and contracted muscles, measured normal to the longitudinal axis of the upper arm at the point of the most prominent biceps muscle – TP

Circumference of the elbow. Circumference at the most dorsal and distal point of the olecranon, with the arm hanging down and the muscles relaxed, measured normal to the longitudinal axis of the upper arm – TP

Maximum forearm circumference. Greatest forearm circumference with the arm hanging down and the muscles relaxed, measured normal to the longitudinal axis of the forearm – TP

Minimal forearm circumference. Lowest forearm circumference with the arm hanging down and the muscles relaxed, measured normal to the longitudinal axis of the forearm near the styloid processes – TP

Wrist circumference. Minimum circumference of the forearm measured at the most distal points of the radial and ulnar styloid processes; the forearm can be raised – TP

Circumference of the base of the thigh. Horizontal circumference of the thigh at the height of the perineum, for balanced weight distribution between feet and a relaxed muscular system – TP

Circumference of the thigh. Greatest horizontal circumference of the thigh for balanced weight distribution between feet and a relaxed muscular system – TP

Lowest circumference of the thigh. Lowest horizontal circumference of the thigh for balanced weight distribution between feet and a relaxed muscular system – TP

Circumference of the knee. Horizontal circumference of the leg at the middle of the patella with a stretched knee – TP

Circumference of the shank. Greatest horizontal circumference of the lower leg – TP

Minimum circumference of the shank. Smallest circumference of the lower leg for balanced weight distribution between feet and a relaxed muscular system – TP

Middle circumference of the foot. Circumference of the unloaded foot kept normal to the lower leg with stretched toes; measured normal to the longitudinal axis of the foot in the middle between the most dorsal point of the heel and the most distal point of the first or second toe (ignoring the toenail) – TP

A.5. Sitting posture (sit.)

Height of seat surface. Linear distance of the surface of the seat from the seat reference surface; with the upper and lower legs so positioned that they formed an angle of 90° – AM

Seated height. Linear distance of the vertex from the seat reference surface for an upright seated posture and orientation of the head in the plane of the eyes and ears – AM

Relaxed seated height. Linear distance of the vertex from the seat reference surface for an relaxed seated posture and orientation of the head in the plane of the eyes and ears – AM

Height to the acromion sit. Linear distance of the most lateral point of the acromion from the seat reference surface in upright seated posture and with the head orientated in the plane of the eyes and ears – AM

Inferior height of the scapula sit. Linear distance of the inferior angle of the scapula from the seat reference surface – AM

Height of the waist sit. Linear distance of the most medial point of the lateral curvature of the trunk in the area of the transversus abdominis muscle from the seat reference surface – AM

Height of the umbilicus sit. Linear distance of the middle of the umbilicus from the seat reference surface – AM

Height of the pelvis sit. Linear distance of the most proximal part of the iliac crest from the seat reference surface – AM

Height C7 sit. Linear distance of the most dorsal point of the spinous process of the seventh cervical vertebra from the seat reference surface – AM

L3 Height sit. Linear distance of the most dorsal point of the spinous process of the third lumbar vertebra from the seat reference surface – AM

L4 Height sit. Linear distance of the most dorsal point of the spinous process of the fourth lumbar vertebra from the seat reference surface – AM

L5 Height sit. Linear distance of the most dorsal of point of the spinous process of the fifth lumbar vertebra from the seat reference surface – AM

Iliospinal height sit. Linear distance of the furthest ventrally and distally directed point of the anterior superior iliac spine from the seat reference surface – AM

Height of the elbow joint sit. Linear distance of the most proximal part of the head of the radius from the seat reference surface, downward stretched arm – AM

Height of the iliac crest sit. Linear distance of the most cranial part of the iliac crest from the reference surface from the seat reference surface – AM

Height of the edge of the thigh Linear vertical distance from the seat reference surface to the highest point on the surface of the right thigh – AM

Height of the knee sit. Linear vertical distance from reference surface to the highest point of the distal lateral part of the femur on the upper side of the right thigh when this is held at a right angle to the lower leg – AM

Greatest width across the hips sit. Greatest linear horizontal distance between the furthest laterally projecting points in the area of the thighs and the hips – BC

Greatest sagittal diameter of the abdomen sit. Projected linear horizontal distance from the furthest dorsally projecting point in the area of the buttocks to the furthest ventrally forward curved point of the abdomen – BC

Buttocks–knee–length Projected linear horizontal distance from the furthest dorsally projecting point in the area of the buttocks to the furthest distally projecting point on the right patella – AM

References

[1] Bradford FK, Spurling RG. The intervertebral disc. In: Charles C. Thomas, Springfield, 1945.

[2] Morris JM, Lucas DB, Bresler B. Role of the trunk in stability of the spine. J Bone Jt Surg [Am] 1961;42-A(3):327–51.

[3] Chaffin D. A computerised biomechanical models – development and use in studying gross body actions. J Biomech 1969;2:429–41.

[4] McGill SM, Norman RW. Dynamically and statically determined low back moments during lifting. J Biomech 1985;18(12):877–85.

[5] McGill SM, Norman RW. Partitioning of the L4-L5 dynamic moment into disc, ligamentous and muscular components during lifting. Spine 1986;11(7):666–78.

[6] McGill SM. Estimation of force and extensor moment contributions of the disc and ligaments at L4/L5. Spine 1988;13:1395–402.

[7] Dieen JJv, Creemers M, Draisma I, Toussaint HM. Repetitive lifting and spinal shrinkage, effects of age and lifting technique. Clin Biomech 1994;9:367–74.

[8] Looze MPd, Kingma I, Thunissen W, Wijk van MJ, Toussaint HM. The evaluation of a practical model estimating lumbar moments in occupational activities. Ergonomics 1994;38:1993–2006.

[9] Deuretzbacher G, Rehder U. A CAE (computer aided engineering) approach to dynamic whole body modeling – the forces in the lumbar spine in asymmetrical lifting. Biomed Tech (Berl) 1995;40(4):93–8.

[10] Morlock M, Bonin V, Schneider E. Biomechanische Untersuchungen zur Quantifizierung der Belastung der Wirbelsäule im Pflegeberuf. In: Wolter D, Seide, K., editors. Berufsbedingte Erkrankungen der Lendenwirbelsäule. Springer, 1998:104–136.

[11] Gagnon D, Gagnon M. The influence of dynamic factors on triaxial net muscular moments at the L5/S1 joint during asymmetrical lifting and lowering. J Biomech 1992;25(8):891–901.

[12] Marras WS, Sommerich CM. A three-dimensional motion model of laods on the lumbar spine: I. Model structure. Hum Factors 1991;33:123–37.

[13] Hughes RE, Bean JC, Chaffin DB. Evaluating the effect of co-contraction in optimization models. J Biomech 1995;28(7):875–8.

[14] Jager M, Luttmann A. The load on the lumbar spine during asymmetrical bi-manual materials handling. Ergonomics 1992;35(7–8):783–805.

[15] Hughes RE, Chaffin DB. The effect of strict muscle stress limits on abdominal muscle force predictions for combined torsion and extension loadings. J Biomech 1995;28(5):527–33.

[16] Plamondon A, Gagnon M, Gravel D. Moments at the L5/S1 joint during asymmetrical lifting: effects of different load trajectories and initial load positions. Clin Biomech 1995;10(3):128–36.

[17] Cappozzo A. Compressive loads in the lumbar vertebral column during normal level walking. J Orthop Res 1984;1:292–301.

[18] Khoo BC, Goh JC, Bose K. A biomechanical model to determine lumbosacral loads during single stance phase in normal gait. Med Eng Phys 1995;17(1):27–35.

[19] Cromwell R, Schultz AB, Beck R, Warwick D. Loads on the lumbar trunk during level walking. J Orthop Res 1989;7(3):371–7.

[20] Shirazi-Adl A. Strain in fibers of a lumbar disc. Analysis of the role of lifting in producing disc prolapse. Spine 1989;14(1):96–103.

[21] Shirazi-Adl A. Finite-element evaluation of contact loads on facets of an L2-L3 lumbar segment in complex loads. Spine 1991;16(5):533–41.

[22] Shirazi-Adl A. Nonlinear stress analysis of the whole lumbar spine in torsion– mechanics of facet articulation. J Biomech 1994;27(3):289–99.

[23] Goel VK, Komg W, Han JS, Weinstein JN, Gilbertson L. A combined finite element and optimization investigation of lumbar spine mechanics with and without muscles. Spine 1993;18(11):1531–41.

[24] Lavaste F, Skalli W, Robin S, Roy-Camille R, Mazel C. Three-dimensional Geometrical and Mechanical Modelling of the Lumbar Spine. J Biomech 1992;25(10):1153–64.

[25] Roy-Camille R, Saillant G, Lavaste F. Experimental study of lumbar disc replacement. Rev Chir Orthop Reparatr Appar Mot (Suppl II) 1978;64:106–7.

[26] Pankoke S, Buck B, Wölfel HP. Dynamic FE model of sitting man adjustable to body height, body mass and posture used for calculating internal forces in the lumbar vertebral disks. J Sound Vib 1998;215:817–39.

[27] Seidel H, Blüthner R, Hinz B, Schust M. On the health-risk of the lumbar spine due to whole-body vibration - theoretical approach, experimental data and evaluation of whole-body vibration. J Sound Vib 1998;215:723–41.

[28] Parnianpour M, Wang JL, Shirazi-Adl A, Sparto P, Wilke H-J. The effect of variations in trunk models in predicting muscle strength and spinal loading. J Musculoskeletal Res 1997;1:55–69.

[29] Shirazi-Adl A, Parnianpour M. Role of posture in mechanics of the lumbar spine in compression. J Spinal Disord 1996;9(4):277–86.

[30] Pope MH. Biomechanics of the lumbar spine. Ann Med 1989;21(5):347–51.

[31] Nachemson A. The influence of spinal movements on the lumbar intradiscal pressure and on the tensile stresses in the annulus fibrosus. Acta Orthop Scand 1963;33:183–207.

[32] Nachemson A, Elfstrom G. Intravital dynamic pressure measurements in lumbar discs. A study of common movements, maneuvers and exercises. Scand J Rehabil Med Suppl 1970;1:1–40.

[33] Nachemson A. The effect of forward leaning on lumbar intradiscal pressure. Acta Orthop Scand 1965;35:314–28.

[34] Nachemson A. In vivo discometry in lumbar discs with irregular necleograms. Acta Orthop Scand 1965;36:418–34.

[35] Nachemson A. The load on lumbar disks in different positions of the body. Clin Orthop 1966;45:107–22.

[36] Nachemson A, Morris JM. J Bone Jt Surg. In vivo Measurements of Intradiscal Pressure 1964;46-A(5):1077–92.
[37] Nachemson AL. Disc pressure measurements. Spine 1981; 6(1):93–7.
[38] Wilke H-J, Neef P, Caimi M, Hoogland T, Claes L. New intradiscal pressure measurements in vivo during daily acitivities. Spine 1999;24(8):755–62.
[39] Greil H. Die Definition von Bezugsebenen, Meßpunkten und Meßstrecken als methodische Grundlage der Anthropometrie. Wissenschaftliche Zeitschrift der Humboldt-Universität zu Berlin Reihe Medizin. 1989(38):125–49.
[40] Hatze H. A model for the computational determination of the parameter values of anthropomorphic segments. Pretoria: Graphic Arts Division of the CSIR 1979:1–61.
[41] Tittel K, Wutscherk H. Sportanthropometrie. Leipzig: Johann Ambrosius Barth; 1972.
[42] Seidel H, Beyer H, Blüthner R, et al. Electromyography in back research – assessment of static and dynamic conditions. Dordrecht, Boston, Lancester: Martinus Nijhoff Publishers, 1985. Perren SM SES-h, 1984, Davos, Switzerland. Dordrecht, Boston, Lancester: Martinus Nijhoff Publishers., editors. Biomechanics: Current Interdisciplinary Research Selected Proceedings of the Fourth Meeting of the European Society of Biomechanics in collaboration with the European Society of Biomaterials.
[43] Greil H. The physique of adults – DDR representative cross sectional anthropometrical study 1982/84. Der Körperbau im Erwachsenenalter – DDR-repräsentative anthropologische Querschnittsstudie 1982/84. Berlin Humboldt-Universität: Habilitation 1988:1–280.
[44] Althoff I, Brinckmann P, Frobin W, Sandover J, Burton K. An improved method of stature measurement for quantitative determination of spinal loading. Application of sitting postures and whole body vibration. Spine 1992;17(6):682–93.
[45] Rohlmann A, Bergmann G, Graichen F. Loads on internal spinal fixators measured in different body positions. Eur Spine J 1999; 8(5):354–9.
[46] van Deursen D, Wilke H-J, Snijders C, van Deursen L. The direct relation between spinal shrinkage and intradiscal pressure in different postures and exercices. Spine, submitted.
[47] Seidel H, Blüthner R, Hinz B, Schust M. Stresses in the lumbar spine due to whole-body vibration containing shocks, Final Report. Bremerhaven: Wirtschaftsverlag NW, 1997. Schriftenreihe der Bundesanstalt für Arbeitsschutz und Arbeitsmedizin Dortmund/Berlin; vol Forschung Fb 777.
[48] Colombini D, Occhipinti E, Grieco A, Faccini M. Estimation of lumbar disc areas by means of anthropometric parameters. Spine 1989;14(1):51–5 [Published erratum appears in Spine 1989 May;14(5):533].
[49] Gruber K, Ruder H, Denoth J, Schneider K. A comparative study of impact dynamics: wobbling mass model versus rigid body models. J Biomech 1998;31(5):439–44.
[50] McNally DS, Adams MA. Internal intervertebral disc mechanics as revealed by stress profilometry. Spine 1992;17(1):66–73.
[51] Adams MA, McNally DS, Wagstaff J, Goodship AE. Abnormal stress concentrations in lumbar intervertebral discs following damage to vertebral bodies: A cause of disc failure. Eur Spine J 1993;1:214–21.
[52] Schultz AB, Andersson GB. Analysis of loads on the lumbar spine. Spine 1981;6:76–82.
[53] Schultz A, Andersson G, Ortengren R, Haderspeck K, Nachemson A. Loads on the lumbar spine. Validation of a biomechanical analysis by measurements of intradiscal pressures and myoelectric signals. J Bone Joint Surg Am 1982;64:713–20.